

# Adsorption Isotherm, Kinetic, and Thermodynamic Studies for Methylene Blue from Aqueous Solution by Needles of *Pinus Sylvestris* L.

Nese Ertugay, Emine Malkoc\*

Department of Environmental Engineering, Ataturk University, Erzurum, Turkey

Received: 9 July 2013

Accepted: 6 March 2014

## Abstract

The adsorption characteristics of methylene blue (MB) onto needles of *Pinus sylvestris* L., an unconventional bio-adsorbent, were investigated. Maximum removal of MB was found to occur at initial pH 5. Adsorption capacity increased from 84.46 to 99.73 mg/g with an increase in temperature from 20 to 45°C at 200 mg/L of initial MB concentration. Adsorption isotherms were modeled with the Langmuir, Freundlich, Tempkin and Harkis-Jura adsorption isotherms. The data fit well with the Langmuir isotherm. The maximum monolayer adsorption capacity of *Pinus sylvestris* L. needles was found to be 101 mg/g at 45°C. The adsorption kinetics of pseudo first-order, pseudo second-order, and Bangham were used for the kinetic studies. The pseudo second-order kinetic model provided the best fit to the experimental data compared with other kinetic adsorption models. Thermodynamic parameters such as  $\Delta G^\circ$ ,  $\Delta H^\circ$ , and  $\Delta S^\circ$  were calculated. The adsorption of MB increased with increasing temperature and thermodynamic parameters, suggesting that the adsorption is spontaneous and endothermic in nature. FTIR spectrum result revealed the presence of adsorbing groups such as carboxyl, hydroxyl, and aromatic-CN stretching in the needles of *Pinus sylvestris* L. The experimental data obtained in the present study indicate that needles of *Pinus sylvestris* L. are suitable candidates for use as adsorbents in the removal of MB.

**Keywords:** methylene blue, needles of *Pinus sylvestris* L., adsorption, kinetic, thermodynamic, isotherm, Bangham equation

## Introduction

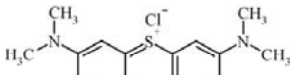
A very small amount of dye in water is highly visible. Discharging even a small amount of dye into water can affect aquatic life and food webs due to the carcinogenic and mutagenic effects of synthetic dyes. Therefore, the removal of dyes from waste effluents is always widely focused [1]. Various treatment methods have been developed for decontamination purposes including coagulation,

chemical oxidation, membrane separation, electrochemical process, and adsorption techniques [2]. As synthetic dyes in wastewater cannot be efficiently decolorized by traditional methods, the adsorption of synthetic dyes on inexpensive and efficient solid supports was considered as a simple and economical method for their removal from water and wastewater. Methylene Blue (MB) is the most commonly used substance for dyeing cotton, wood, and silk. It can cause eye burns that may be responsible for permanent injury to the eyes of humans and animals. On inhalation, it can give rise to short periods of rapid or difficult breathing while inges-

---

\*e-mail: emalkoc@atauni.edu.tr

Table 1. Physicochemical properties of the MB dye.

Color Index Name	Basic Blue 9
Molecular Formula	C <sub>16</sub> H <sub>18</sub> ClN <sub>3</sub> S
Molecular weight (g/mol)	319.9
$\lambda_{max}$ (nm)	664
Molecular structure [7]	

tion through the mouth produces a burning sensation and may cause nausea, vomiting, profuse sweating, mental confusion, and methemoglobinemia [3, 4]. Therefore, the treatment of effluent containing such dye is of interest due to its harmful impacts on receiving waters [3].

Used in this study, *Pinus sylvestris* L. is an evergreen coniferous tree that is readily identified by its combination of fairly short, blue-green leaves and orange-red bark. The shoots are light brown, with a spirally arranged scale-like pattern. On mature trees the leaves ('needles') are a glaucous blue-green, often darker green to dark yellow-green in winter [5]. Evergreen needles are 1.5 to 3 inches long, with two stout, twisted needles per fascicle, blue-green with distinct stomatal bands [6].

This study aimed to gain an understanding of the adsorption kinetics, to describe the mechanism of adsorption, to determine the factors controlling the rate of adsorption, and to calculate the thermodynamic parameters of the system. The effects of solution pH, concentration, adsorbent dosage, and temperature on MB adsorption rate have been investigated.

## Materials and Methods

### Materials

Needles of *Pinus sylvestris* L. needles were collected in March 2011 from the garden of Engineering Faculty at Ataturk University. Fresh needles of *Pinus sylvestris* L. were dried at 80°C for 48 h and cut into small pieces. Adsorption experiments were carried out 250+500  $\mu$ m at adsorbent particle size.

### Methylene Blue (MB)

In this study Methylene Blue (E. Merck, Darmstadt), a commercial azo dye, was used. Physicochemical properties of methylene blue were shown in Table 1.

### Batch Adsorption Experiments

Adsorption experiments were carried out in 250 mL erlenmeyer flasks containing a determined amount MB on a rotary shaker at 150 rpm at 20°C. The samples were taken

at definite time intervals (at 1,3, 5, 10, 15, 20, 30, and 45 min) and were filtered immediately to remove biomass with filter paper (Whatman 42). The final filtrate concentrations of MB in the solution were measured at maximum wavelengths of MB (664 nm) using a double-beam UV/vis spectrophotometer (Shimadzu UV-160A). The amount of MB adsorbed was calculated by defining the difference between the initial MB concentration and the concentration of the solution during the sampling.

## Results and Discussion

### Influence of Initial Solution pH on MB Adsorption by Needles of *Pinus sylvestris* L.

The aqueous solution pH is expected to influence the adsorptive uptake of dyes due to its impact on both the surface-binding sites of the adsorbent and the ionization process of the dye molecule [8]. The effect of pH on the adsorption of MB at equilibrium ( $q_e$ ) and efficiency removal by needles of *Pinus sylvestris* L. are shown in Fig. 1.

At low pH values,  $q_e$  values also are low. This is due to the cationic dye reaction with OH<sup>-</sup>. Acidic conditions produce more H<sup>+</sup> ions in the system. The surface of the adsorbent gathers positive charges by absorbing H<sup>+</sup> ions, which prevent the adsorption of dye ions onto adsorbent surface due to electrostatic repulsion and the competition between H<sup>+</sup> ions and MB for the adsorption sites [9, 10]. In contrast, when the pH values increased, adsorbent surfaces were more negatively charged with subsequent attraction of dye ions with positive charge and the adsorption process was favored until a maximum was reached around pH 5. Decrease in adsorption at higher pH may be due to the formation of soluble hydroxyl complexes.

As seen in Fig. 1, the percent removal of MB onto needles of *Pinus sylvestris* L. was found to be 55.96, 74.40, 97.70, 97.50 and 87.40% for solutions of pH 3, 4, 5, 7, and 8, respectively. Also, the maximum adsorption capacity of used adsorbent was determined as 39.08 mg/g at pH 5. Thus, all the adsorption experiments were conducted at this

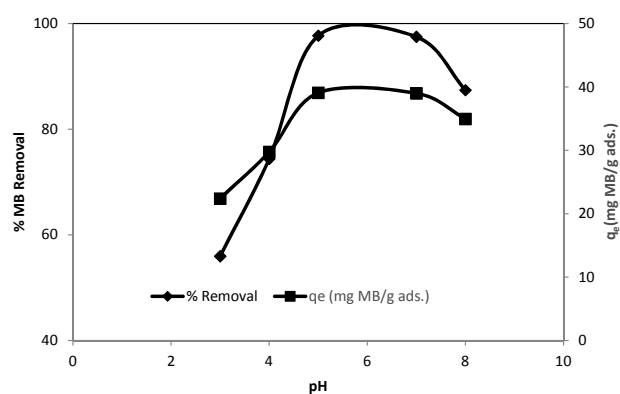


Fig. 1. Effect of pH on the adsorption of MB onto needles of *Pinus sylvestris* L. ( $T = 20^\circ\text{C}$ ,  $C_0 = 100$  mg/L, adsorbent dosage = 0.375 g/200 mL, contact time = 45 min).

optimum pH value. By experiments, the pH of original MB solution was 5.0 and it was not adjusted in other experiments.

### Influence of Initial Dye Concentration on MB Adsorption by Needles of *Pinus sylvestris* L.

The plot of removal yield versus the contact time at various initial MB concentrations was shown in Fig. 2. It was evident from the figure that adsorption equilibrium was established at 45 min.

In this study the adsorption process can be advanced in two phases. The first stage was the rapid initial adsorption within 5 min. A later phase was slow adsorption process within the range of 5-45 min. In the third phase, the adsorption capacity did not vary significantly after 180 min., when the adsorption would be in a state of dynamic equilibrium between the dye desorption and adsorption. The reason is that during the adsorption of dye, initially the dye molecules rapidly reach the boundary layer by mass transfer, then they slowly diffuse from boundary layer film onto the adsorbent surface because many of the available external sites have been occupied and, finally, they diffuse into the porous structure of the adsorbent [9-11].

Fig. 3 shows the adsorption yields and adsorption capacities versus at various initial MB concentrations at room temperature. The amount of MB adsorbed (mgMB/g) increased with increase initial MB concentration. The amount of MB removed at equilibrium increased from 26.51 to 99.73 mg/g with the increase in dye concentration from 50 to 200 mg/L. It is clear that the removal of dye depends on the concentration of the dye. When the initial concentrations increased, the mass transfer driving force became larger and the interaction between MB and adsorbent was enhanced, thus resulting in higher adsorption capacity.

As seen in Fig. 3, when the initial MB concentration was increased from 50 to 200 mg/L, the removal decreased from 99.40 to 79.18%. This was due to the saturation of the sorption sites on the adsorbent as the concentration of the

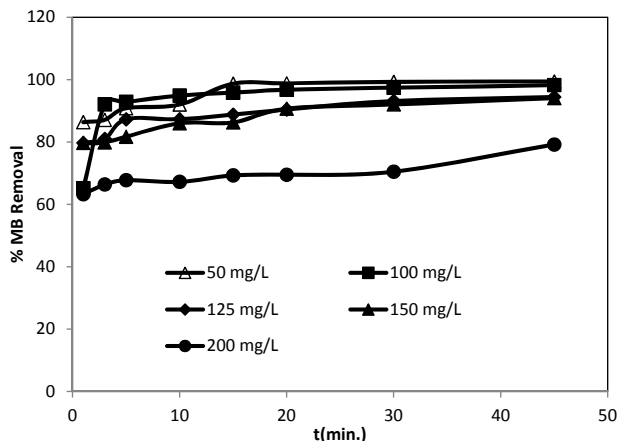


Fig. 2. Effect of initial MB concentration on the adsorption of MB onto needles of *Pinus sylvestris* L. (T = 20°C, pH=5.0, adsorbent dosage = 0.375 g/200 mL).

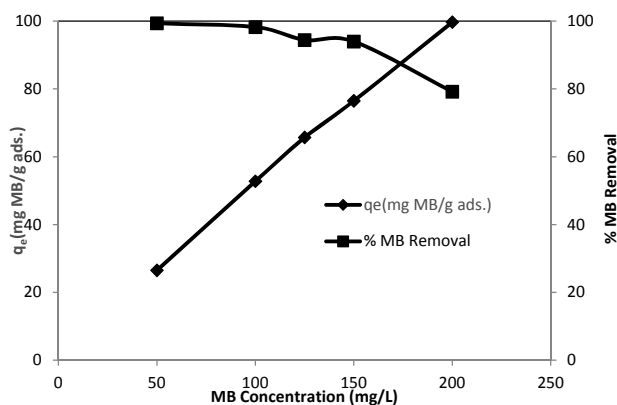


Fig. 3. Effect of initial dye concentration on the adsorption of MB onto needles of *Pinus sylvestris* L. (T = 20°C, pH=5.0, adsorbent dosage= 0.375 g/200 mL, contact time = 45 min).

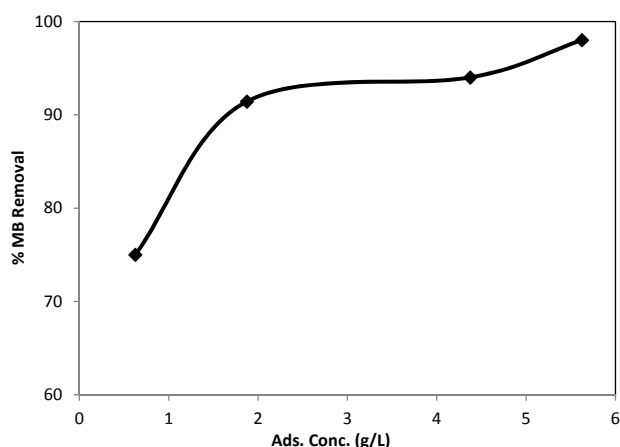


Fig. 4. Effect of adsorbent dosage on the adsorption of MB onto needles of *Pinus sylvestris* L. (T=20°C, pH=5.0, initial dye concentration=200 mg/L, contact time=45 min).

dye increased. However, higher dye adsorption yields were observed at lower dye concentrations.

### Influence of Adsorbent Dosage on MB Adsorption by Needles of *Pinus sylvestris* L.

The influence of adsorbent dosage on the efficiency of MB removal was shown in Fig. 4. Adsorbent dosage varied from 0.625 to 5.625 g/L. The results are presented in Fig. 4, which indicates that the adsorption yield of MB increases with increasing adsorbent doses for 200 mg/L initial MB concentration. When the adsorbent concentration was increased from 0.625 to 5.625 g/L, the removal increased from 75 to 98%. This may be due to the fact that the higher the doses of the adsorbent, the more sorbent surface and pore volume will be available for adsorption [12].

At the same time, the amount of dye adsorbed per unit mass of adsorbent decreased with increasing adsorbent mass due to the reduction in effective surface area. The equilibrium adsorption capacity decreased from 136 to 30 mg/g with the increasing adsorbent dosage from 0.625 to 5.625 g/L. The decrease in adsorption density and the

Table 2. Thermodynamic parameters for the adsorption of MB onto needles of *Pinus sylvestris* L.

MB conc. (mg/L)	$\Delta G^{\circ}$ (kJ/Kmol)			$\Delta H^{\circ}$ (kJ/mol)	$\Delta S^{\circ}$ (J/mol K)
	293 K	308 K	318 K		
100	-9.82	-11.54	-12.09	17.23	0.09
125	-6.90	-8.48	-11.17	41.86	0.16
150	-6.73	-7.25	-8.16	9.56	0.06
200	-3.25	-6.06	-7.05	41.91	0.15

amount of mass adsorbed per unit were due to the splitting effect of flux (concentration gradient) between adsorbates with increasing adsorbent concentration causing a decrease in the amount of dye adsorbed onto unit weight of biomass [13].

#### Influence of Temperature on MB Adsorption by Needles of *Pinus sylvestris* L.

The effect of temperature on the adsorption of MB on needles of *Pinus sylvestris* L. was investigated at 20, 35, and 45°C. The results are shown in Fig. 5. The experimental results demonstrate that the magnitude of adsorption is proportional to the solution temperature (Table 2). The temperature has two major effects on the adsorption process. Increasing the temperature is known to increase the rate of diffusion of the adsorbate molecules across the external boundary layer and in the internal pores of the adsorbent particle, owing to the decrease in the viscosity of the solution for highly concentrated suspensions. In addition, changing the temperature will change the equilibrium capacity of the adsorbent for a particular adsorbate [14].

As seen in Fig. 5, the adsorption of MB on needles of *Pinus sylvestris* L. is increased from 52.41 mg/g (98.26% removal) to 52.79 mg/g (98.98% removal) when temperature was increased from 20 to 45°C at an initial concentration of 100 mg/L.

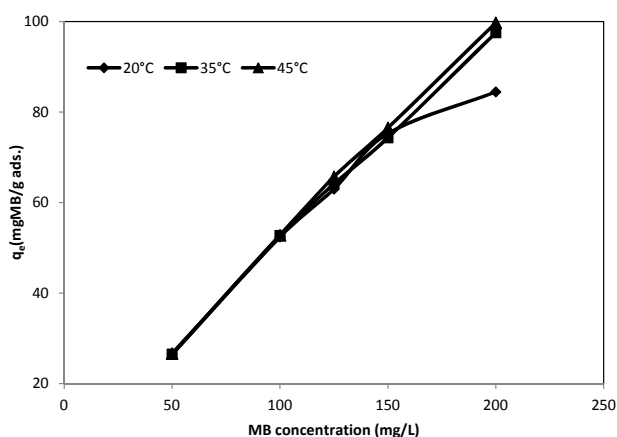


Fig. 5. Effect of temperature on the adsorption of MB onto needles of *Pinus sylvestris* L. (adsorbent dosage=0.375 g/200 mL, pH=5.0, contact time = 45 min).

To determine whether the process will occur spontaneously, a set of thermodynamic parameters for the MB adsorption system by needles of *Pinus sylvestris* L. was calculated, including changes in the standard free energy ( $\Delta G^{\circ}$ ), enthalpy ( $\Delta H^{\circ}$ ), and entropy ( $\Delta S^{\circ}$ ) [15]:

$$\Delta G^{\circ} = -RT \ln K_c \quad (1)$$

...where  $R$  is universal gas constant (8.314 J/(molK)),  $T$  is the temperature (K). The values of  $\Delta H^{\circ}$  and  $\Delta S^{\circ}$  were calculated from the intercept and slope of a plot of  $\Delta G^{\circ}$  versus  $T$  according to Eq. (3) by linear regression analysis (Fig.6).

The apparent equilibrium constant ( $K_c$ ) of the adsorption is defined as [15]:

$$K_c = \frac{C_{ad,eq}}{C_{eq}} \quad (2)$$

...where  $C_{ad,eq}$  and  $C_{eq}$  are the concentrations of MB on the adsorbent and residual MB concentration at equilibrium, respectively. In this case, the activity should be used instead of concentration in order to obtain the standard thermodynamic equilibrium constant ( $K_c$ ) of the adsorption system.

$$\Delta G^{\circ} = \Delta H^{\circ} - T\Delta S^{\circ} \quad (3)$$

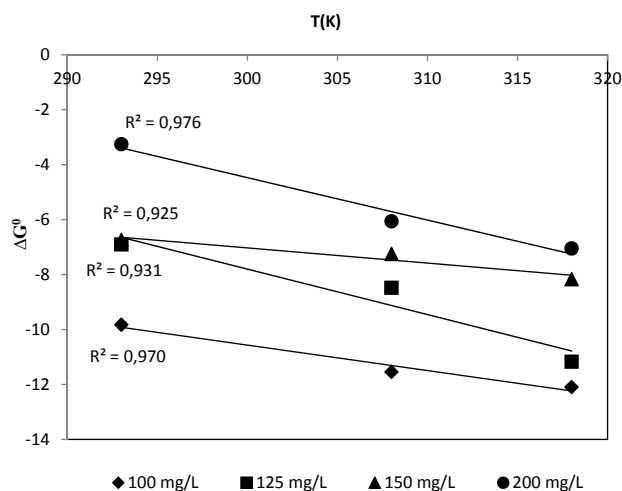


Fig. 6.  $\Delta G^{\circ}$  vs. T for the adsorption of MB onto needles of *Pinus sylvestris* L.

As seen in Table 2, positive values of  $\Delta H^\circ$  (17.23, 41.86, 9.56, 41.91 kJ/mol) show the endothermic nature of adsorption for all MB concentrations. The negative values of  $\Delta G^\circ$  at all MB concentrations indicate the spontaneous nature of adsorption for MB at 20, 35, and 45°C. The positive values of  $\Delta S^\circ$  (0.09, 0.16, 0.06, 0.15 J/mol K) suggest the increased randomness at the solid/solution interface during the adsorption of MB on needles of *Pinus sylvestris* L.

### Adsorption Kinetics of MB Adsorption by Needles of *Pinus sylvestris* L.

The rate constants were calculated by using pseudo first-order and pseudo second-order kinetic models.

The pseudo first-order model of Lagergren is based on the assumption that the rate of change of adsorbed solute with time is proportional to the difference in equilibrium adsorption capacity and the adsorbed amount. The pseudo first-order equation is expressed as follows [9, 15]:

$$\log(q_e - q_t) = \log q_e - \frac{k_1}{2.303} t \quad (4)$$

...where  $q_t$  (mg/g) is the amount of adsorbed MB on the adsorbent at time  $t$ , and  $k_1$  (1/min) is the rate constant of first-order adsorption. A straight line of  $\log(q_e - q_t)$  versus  $t$  suggests the applicability of this kinetic model and is shown in Figs. 7a, b, and c.  $q_e$  and  $k_1$  can be determined from the intercept and slope of the plot, respectively.

The linearized form of the pseudo-second order kinetic expression [16] is represented by Eq. (5).

$$\frac{t}{q_t} = \frac{1}{k_2 q_e^2} + \frac{1}{q_e} t \quad (5)$$

...where  $k_2$  (g/(mg·min)) is the rate constant of second order adsorption and  $q_e$  and  $q_t$  are amounts of dye sorbed (mg/g) at equilibrium and at any time ( $t$ ), respectively. The plot  $t/q_t$  versus  $t$  should give a straight line (Figs. 8a, b, c) if second order kinetics are applicable and  $q_e$ ,  $k_2$ , and  $R^2$  can be determined from the slope and intercept of the plot, respectively.

The initial adsorption rate,  $h$  (mol/(g min)) is expressed as:

$$h = k_2 q_e^2 \quad (6)$$

...where the initial adsorption rate ( $h$ ), the equilibrium adsorption capacity ( $q_e$ ), and the second-order constants  $k_2$  (g/(mol·min)) can be determined experimentally from the slope and intercept of plot  $t/q_t$  versus  $t$  [14].

Kinetic data can further be used to check whether pore diffusion was the only rate-controlling step or not in the adsorption system using Bangham's equation [17, 18]:

$$\log \log \frac{C_0}{C_0 - q_t m} = \log \frac{K_B m}{2.303 v} + \alpha \log t \quad (7)$$

...where  $C_0$  is initial concentration of adsorbate in solution (mg/L),  $v$  the volume of solution (mL),  $m$  the weight of

adsorbent used per litre of solution (g/L),  $q_t$  (mg/g) the amount of adsorbate retained at time  $t$ , and  $\alpha$  (<1), and  $K_B$  are constants. As such,  $\log \log \frac{C_0}{C_0 - q_t m}$  values were plotted against  $\log t$  in Figs. 9a, b, c at different temperatures.

Table 3 provides pseudo first-order rate constants  $k_1$ , pseudo second-order rate constants  $k_2$ ,  $h$ , calculated equilibrium sorption capacity  $q_{e,the}$  (theoretical), and experimental equilibrium sorption capacity  $q_{e,exp}$  (experimental) at various initial MB concentrations and temperatures.

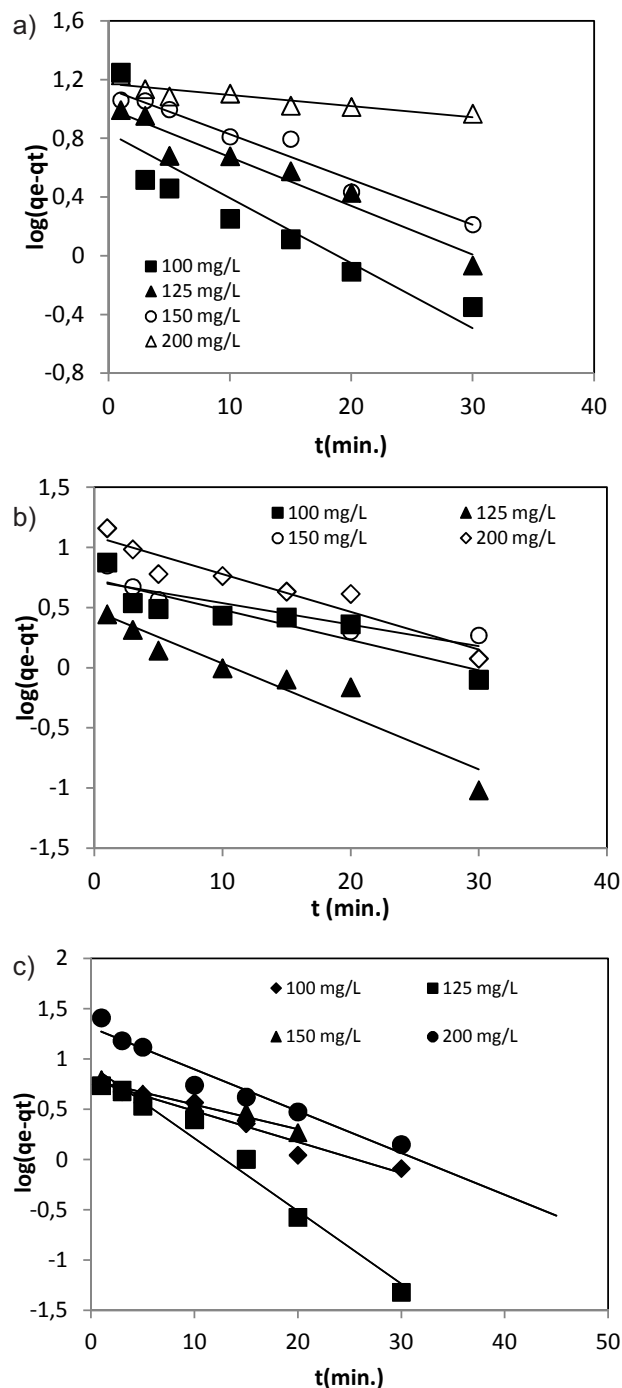


Fig. 7. Pseudo first-order kinetics for adsorption of MB dye onto needles of *Pinus sylvestris* L. a) 20°C, b) 35°C, c) 45°C (adsorbent dosage=0.375 g/200 mL, pH=5.0, contact time = 45 min.).

Also, kinetic datas can further be used to check whether pore diffusion is the only rate controlling step or not in the adsorption system using Bangham's equation given in Table 3. If the experimental datas represented by this equation then the adsorption kinetics are limited by the pore diffusion. Kinetic parameters and the correlation coefficients obtained by Bangham's equation are given in Table 3 and the data are exploring poorer fit of the model. This situation represents that the diffusion of adsorbate into pores of the sorbent is not the only rate-controlling step [19].

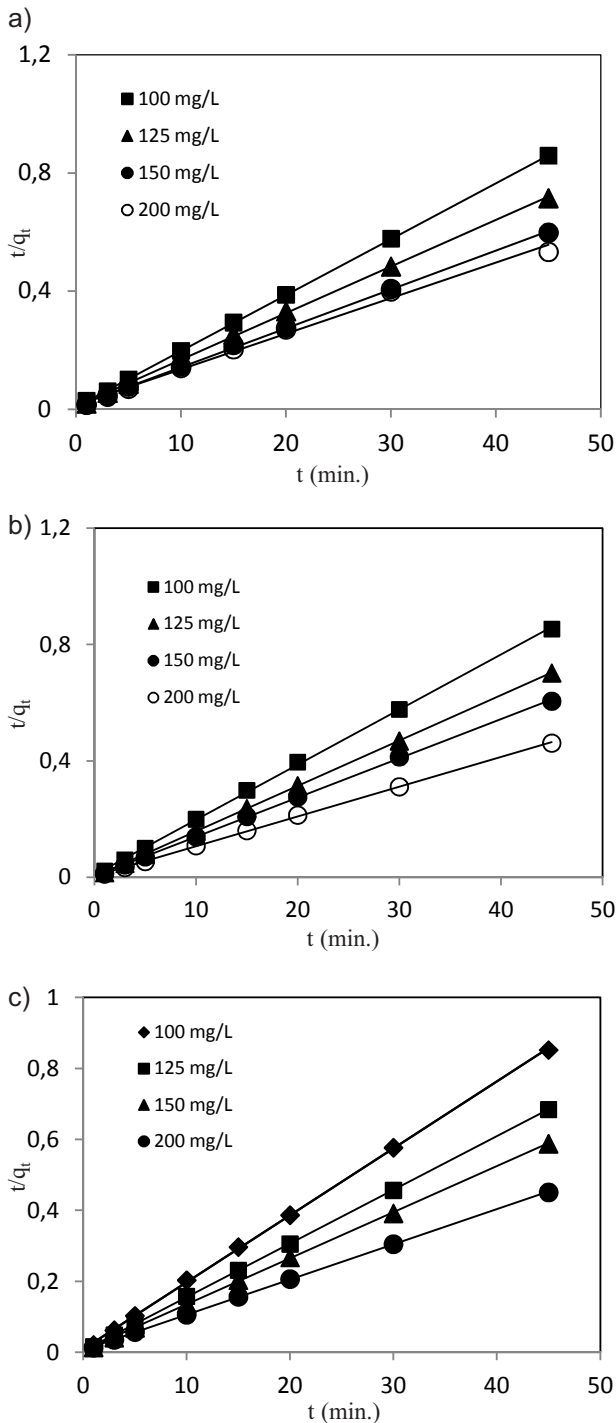


Fig. 8. Pseudo second-order kinetics for adsorption of MB dye onto needles of *Pinus sylvestris* L. a) 20°C, b) 35°C, c) 45°C (adsorbent dosage=0.375 g/200 mL, pH=5.0, contact time = 45 min.)

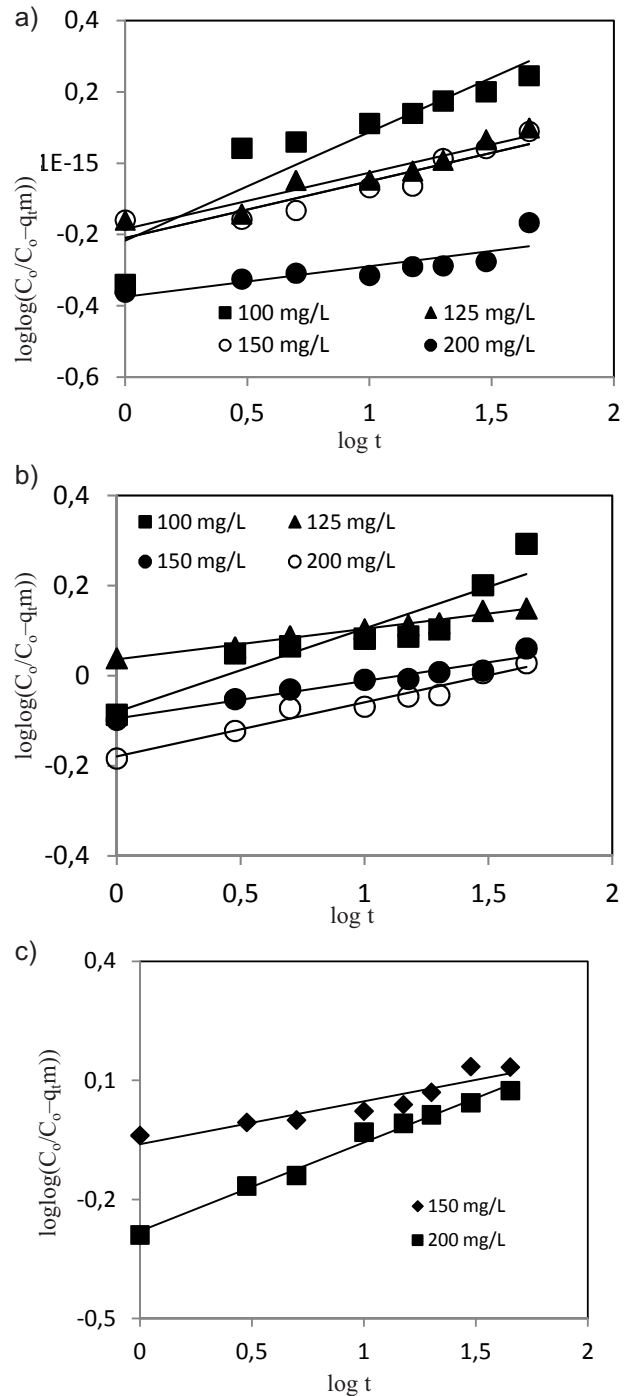


Fig. 9. Bangham equation for adsorption of MB dye onto needles of *Pinus sylvestris* L. a) 20°C, b) 35°C, c) 45°C (adsorbent dosage=0.375 g/200 mL, pH=5.0, contact time=45 min.)

The validity of the kinetic models is tested by the magnitude of the regression coefficient  $R^2$  given in Table 3. It is important to note that for a pseudo first-order model, the correlation coefficient is less than 0.98, which is indicative of a bad correlation. The first-order model did not provide a good fit, with  $q_e$  values being significantly underestimated. Also in this manner, the interaction of MB on needles of *Pinus sylvestris* L. present a complex behavior, when the traditional pseudo-first order model seem not to be enough or satisfactory to explain the kinetic data.

Table 3. A comparison of the pseudo first-order kinetic and pseudo second-order kinetic rate constants and theoretical and experimental  $q_e$  values obtained at different initial MB concentrations and temperatures.

MB conc. (mg/L)	$q_{e,exp}$ (mg/g)	Pseudo First-Order Kinetic			Pseudo Second-Order Kinetic				Bangham Equation		
		$q_{e,cal}$ (mg/g)	$k_1$ (L/min)	$R^2$	$q_{e,cal}$ (mg/g)	$k_2$ (mg/gmin)	$R^2$	$h$ (mg/gmin)	$k_B$ (L/g)	$\alpha$	$R^2$
20°C											
100	52.41	6.86	1.020	0.8033	52.90	0.046	1.0000	128.73	0.149	0.304	0.8482
125	62.97	10.11	0.076	0.9399	63.29	0.025	0.9995	100.14	0.161	0.157	0.9240
150	75.27	13.67	0.071	0.9619	75.76	0.017	0.9993	97.57	0.152	0.159	0.8705
200	84.46	14.84	0.018	0.8113	83.33	0.010	0.9931	68.74	0.104	0.085	0.6925
35°C											
100	52.75	5.41	0.058	0.8279	52.90	0.042	0.9996	117.50	0.204	0.185	0.8493
125	64.07	2.97	0.101	0.9187	64.10	0.116	1.0000	476.15	0.266	0.068	0.9800
150	74.34	5.22	0.041	0.8115	74.08	0.041	0.9997	227.30	0.197	0.083	0.9483
200	97.52	12.34	0.072	0.9108	98.04	0.020	0.9997	196.09	0.163	0.119	0.9608
45°C											
100	52.79	6.20	0.071	0.9573	53.19	0.039	0.9997	109.89	-	-	-
125	65.71	8.61	0.166	0.9748	66.22	0.057	1.0000	250.00	-	-	-
150	76.51	6.16	0.056	0.9654	76.92	0.035	0.9998	208.32	0.214	0.108	0.8706
200	99.73	20.55	0.096	0.9529	101.00	0.015	0.9999	151.48	0.129	0.223	0.9867

Values of  $k_1$ ,  $k_2$ ,  $q_{e,cal}$  and  $R^2$  along with calculated linear correlation coefficients for the two models are shown in Table 3. As can be seen in Table 3, the correlation coefficients calculated from the pseudo second-order model were very high (>0.99) for all MB concentrations and temperatures. At the same time, the calculated  $q_e$  values from the pseudo second order model were in good agreement with the experimental  $q_e$  values calculated from the pseudo second-order kinetic model. Thus, it can be inferred that the rate-limiting step may be chemisorption promoted by either valency forces, through sharing of electrons between adsorbent and sorbate, or covalent forces, through the exchange of electrons between the parties involved [8].

### Adsorption Isotherms of MB Adsorption by Needles of *Pinus sylvestris* L.

The adsorption isotherm indicates how the adsorption molecules distribute between the liquid phase and the solid phase when the adsorption process reaches an equilibrium state. The analysis of the isotherm datas by fitting them to different isotherm models is an important step to find the suitable model that can be used for design purposes [20]. Table 4 shows the Freundlich, Langmuir, Tempkin, and Harkins Jura equations and parameters of these isotherms.

In order to assess different isotherms (Freundlich, Langmuir, Tempkin, Harkins Jura) and their ability to correlate with experimental results, the fitted plots from each

Table 4. The names and non-linear forms of studied adsorption isotherms (Freundlich, Langmuir, Tempkin, Harkins-Jura).

Freundlich	$q_e = K_f C_e^{1/n}$
Langmuir	$q_e = \frac{Q_0 b C_e}{1 + b C_e}$
Tempkin	$q_e = \frac{RT}{b_T} \ln (A C_e)$
Harkins-Jura	$q_e = \left( \frac{A_{HJ}}{B_{HJ} - \log C_e} \right)^{1/2}$

isotherm were shown with the experimental data for adsorption of MB onto needles of *Pinus sylvestris* L. at 20, 35, and 45°C in Figs. 10 a, b, c, and d.

As seen from Figs. 10 a-d and Table 5, the adsorption of MB dye onto needles of *Pinus sylvestris* L. at different temperatures fits quite well into the Langmuir adsorption model. Maximum adsorption capacity of needles of *Pinus sylvestris* L. was found 101 mg/g at 45°C, indicating physical monolayer adsorption. The fact that the Langmuir isotherm fits the experimental data very well may be due to homogenous distribution of active sites on the adsorbent surface; since the Langmuir equation assumes that the surface is homogenous [21].

Moreover,  $Q_0$  and  $b$  increased with increasing temperature, as shown in Table 5.  $b$  value represents the equilibri-

um adsorption constant and relates to adsorption heat, therefore a higher value of  $b$  indicates a favorable adsorption process [9]. As for the Freundlich, Tempkin, and Harkins-Jura equations the poor fit to the experimental data as well as its empirical nature does not allow for reliable assumptions. The Freundlich parameter  $1/n$  relates to surface heterogeneity. When  $0 < 1/n < 1$ , the adsorption is favorable;  $1/n=1$ , the adsorption is homogeneous and there is no interaction among the adsorbed species;  $1/n > 1$ , the adsorption is unfavorable [22]. It has been known that the magnitude of  $K_F$  indicates a measure of the adsorbent capacity [23]. As indicated in Table 5, the values of the exponent  $1/n$  were in the range of 0-1, indicating favourable adsorption.

The essential characteristics of Langmuir isotherm can be expressed by a dimensionless constant called equilibrium parameter  $R_L$ , defined by [20, 23]:

$$R_L = \frac{1}{1 + bC_0} \tag{8}$$

...where  $b$  is the Langmuir constant and  $C_0$  (mg/L) is initial MB concentration. The value of  $R_L$  indicates the type of the

isotherm to be either unfavorable ( $R_L > 1$ ), linear ( $R_L = 1$ ), favorable ( $0 < R_L < 1$ ), or irreversible ( $R_L = 0$ ). The values of  $R_L$  calculated according to Eq. (8) were found to be within the range of 0-1. The results given in Fig. 11 show that the adsorption of MB onto needles of *Pinus sylvestris* L. is favorable.

### Fourier Transform Infrared Spectroscopy (FTIR) Analysis

In order to investigate the surface characteristic of needles of *Pinus sylvestris* L., FTIR of needles of *Pinus sylvestris* L. was studied. The FTIR characteristics are shown in Figs. 12 a, b, and Table 6.

As seen in Table 6, the FTIR spectroscopic analysis indicated broad bands at 3,340  $\text{cm}^{-1}$ , 2,923  $\text{cm}^{-1}$ , and 1,733  $\text{cm}^{-1}$  representing bonded -OH groups, aliphatic C-H group, and C=H group, respectively. The bands observed at about 1657-1621  $\text{cm}^{-1}$  could be assigned to the aliphatic C=O stretching. The peaks around 1,539  $\text{cm}^{-1}$  and 1,445  $\text{cm}^{-1}$  correspond to the secondary amine group and carboxylate groups. Carboxyl groups, C-O stretching of ether groups, and -C-C- groups are observed to shift to 1,371-1,314  $\text{cm}^{-1}$ ,

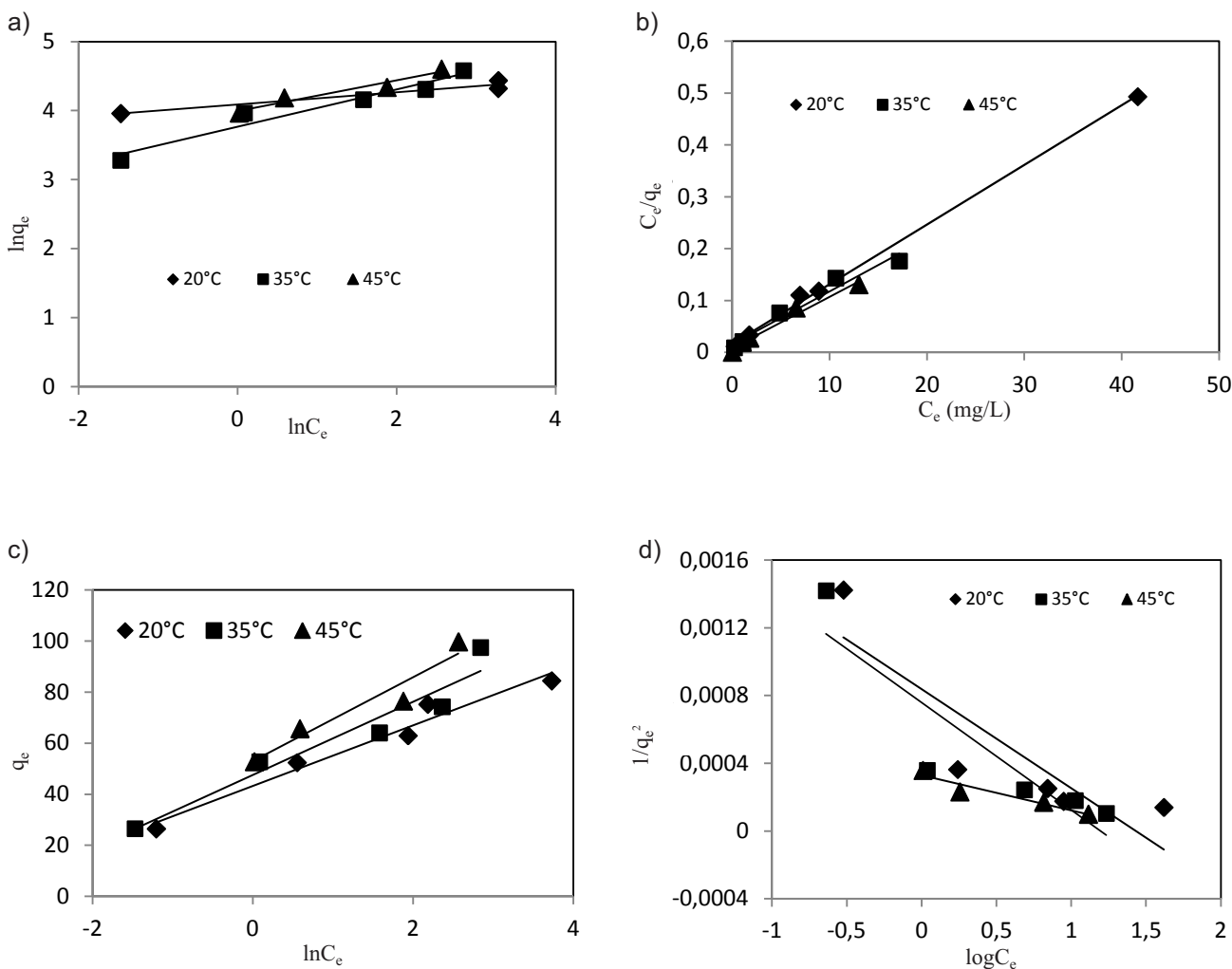


Fig. 10. Adsorption isotherms at different temperatures; adsorption of MB onto needles of *Pinus sylvestris* L. a) Freundlich, b) Langmuir, c) Tempkin, d) Harkins-Jura.



Table 5. Isotherm constants for MB onto needles of *Pinus sylvestris* L.

Adsorption Isotherms	Temperatures		
	20°C	35°C	45°C
Langmuir isotherm			
$Q_0$ (mg/g)	86.96	98.04	101.00
$b$ (L/g)	0.65	0.71	1.19
$R^2$	0.9981	0.9626	0.9768
Freundlich isotherm			
$K_f$ (L/g)	60.77	43.25	54.11
$1/n$	0.085	0.270	0.223
$R^2$	0.9354	0.9463	0.9458
Tempkin isotherm			
$A$ (L/g)	38.00	27.59	24.97
$b_T$	11.88	14.34	16.45
$R^2$	0.9654	0.9315	0.9287
Harkins-Jura			
$A_{HJ}$	1666.67	2000.00	5000.00
$B_{HJ}$	1.33	1.40	1.50
$R^2$	0.7665	0.8011	0.9139

1,155-1,105  $\text{cm}^{-1}$ , and 1,064-1,037  $\text{cm}^{-1}$ , respectively. The peaks observed at 894  $\text{cm}^{-1}$  and 535  $\text{cm}^{-1}$  correspond to aromatic -CH stretching. The bands observed at about 669-614  $\text{cm}^{-1}$  could be assigned to the -CN stretching.

Among these absorption peaks especially the aromatic -CN stretching [24, 25], bonded -OH groups, C=O stretching, -C-C-group [26], C-O stretching of ether groups [27], and carboxyl groups were especially involved in MB adsorption.

Carboxyl and hydroxyl groups may function as proton donors; hence deprotonated hydroxyl and carboxyl groups may be involved in coordination with metal ions and action with positive dye ions [28].

### Comparison of *Pinus sylvestris* L. Needles with Other Adsorbents

Many researchers have investigated several adsorbents for the removal of MB from aqueous solutions. Table 7 lists the comparison of maximum monolayer adsorption capacity of MB onto various adsorbents. It is clear that needles of *Pinus sylvestris* L. used in this work had a relatively suitable adsorption capacity of 86.96 mg/g if compared to other adsorbents found in the literature, with three exceptions [16, 29, 30], than reported elsewhere. This suggests that MB could be easily adsorbed onto needles of *Pinus sylvestris* L.

Table 6. FTIR of needles of *Pinus sylvestris* L. before and after MB adsorption.

Frequency (1/cm)		Differences (1/cm)	Assignment
Before	After		
3340	3412	-72	Bonded OH groups
2923	2917	6	Aliphatic C-H group
1733	1736	-3	C=H group
1657	1648	9	C=O stretching
1621	1596	25	C=O stretching
1539	1533	6	Secondary amine group
1445	1443	2	Carboxylate groups
1371	1382	-11	Carboxyl groups
1338	1349	-11	Carboxyl groups
1314	1327	-13	Carboxyl groups
1155	1168	-13	C-O stretching of ether groups
1105	1102	3	C-O stretching of ether groups
1064	1056	8	-C-C- group
1037	1031	6	-C-C- group
894	883	11	Aromatic -CH stretching
669	666	3	-CN stretching
614	609	5	-CN stretching
535	582	-47	Aromatic -CH stretching

### Conclusions

Experiments were conducted to investigate needles of *Pinus sylvestris* L. as adsorbents for the removal of methylene blue (MB) from aqueous solutions. The following conclusions are made based on the results of present study and scientific information derived from literature:

1. Various effective factors such as contact time, adsorbent dose, initial MB concentration, solution pH, and temperature were optimized. The extent of the dye removal increased with increasing the solution temperature and optimum pH value for dye adsorption was observed at pH 5.0 for needles of *Pinus sylvestris* L. The equilibrium of the MB adsorption is reached within about 45 min.
2. The Langmuir, Freundlich, Tempkin, and Harkins-Jura isotherm were employed to discuss adsorption behavior. Equilibrium data were proved to be compatible with the Langmuir isotherm. The maximum monolayer adsorption capacities were found to be 86.96, 98.04 and 101.00 mg/g at 20, 35, and 45°C, respectively.
3. The dimensionless separation factor ( $R_L$ ) showed that WHS can be used for removal of MB from aqueous solutions.

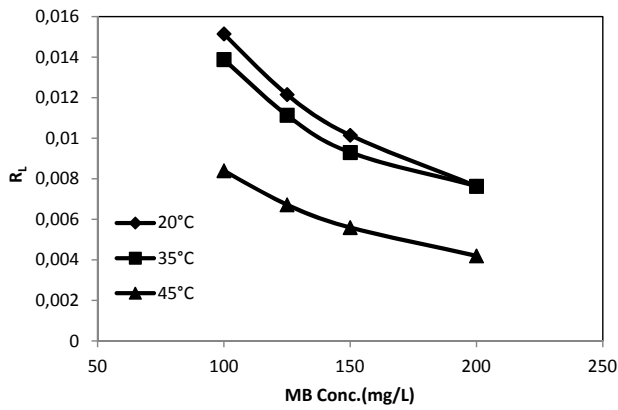


Fig. 11.  $R_L$  values at different temperatures relating to the initial MB concentrations.

- The kinetics of the adsorption process were found to follow the pseudo-second-order kinetic model.
- Negative value of  $\Delta G^\circ$  and positive value of  $\Delta H^\circ$  confirmed the spontaneous and endothermic nature of the adsorption process.
- The electrostatic attraction between bonded  $-\text{OH}$  groups,  $\text{C}=\text{O}$  stretching,  $-\text{C}-\text{C}-$  group, carboxyl groups,  $\text{C}-\text{O}$  stretching of ether groups, and aromatic  $-\text{CN}$  stretching groups and MB can describe the main adsorption process by FTIR spectra before and after adsorption of MB on needles of *Pinus sylvestris* L.
- Needles of *Pinus sylvestris* L., an inexpensive and easily available material, can be an alternative for more costly adsorbents used for MB removal in wastewater treatment processes.

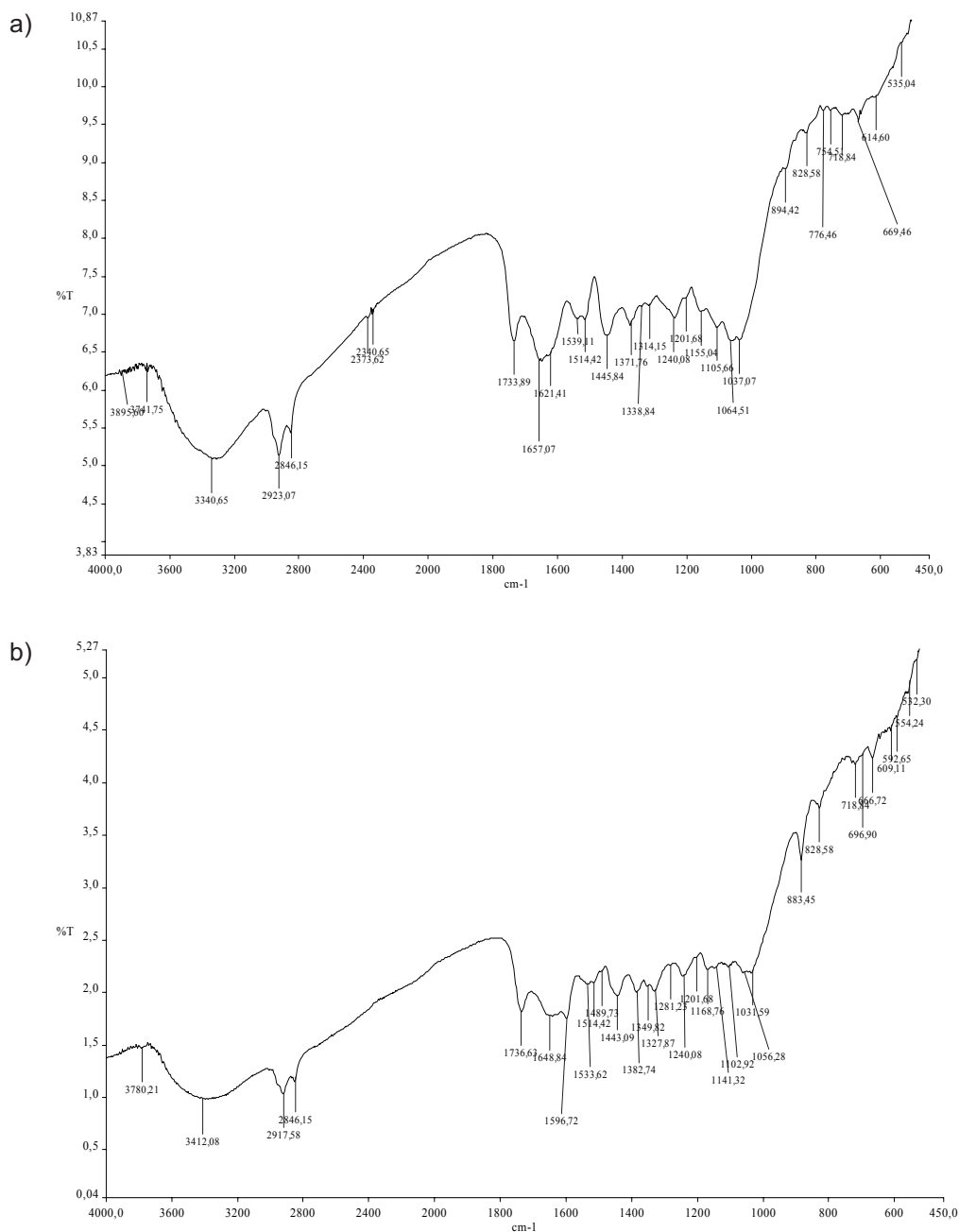


Fig. 12. FTIR spectra of *Pinus sylvestris* L needles (a) and MB-loaded *Pinus sylvestris* L needles (b).

Table 7. Comparison of adsorption capacity of methylene blue on various adsorbents.

Adsorbent	Adsorbent capacity (mg/g)	References
Date pits	80.31	[31]
Jute processing waste	22.47	[32]
Tea waste	85.16	[33]
Phosphoric acid-treated Parthenium (an agricultural waste) carbon (PWC)	88.49	[29]
Banana peel	20.8	[34]
Cereal chaff	20.3	[35]
Wheat shells	16.56	[36]
Natural zeolite	19.94	[37]
NaOH-modified rejected tea	242.11	[16]
NaOH-treated raw koalin	16.34	[38]
NaOH-treated pure koalin	20.49	[38]
Activated carbon from Egyptian rice hull	60.10	[39]
Coffee husks	90.1	[30]
Rice husks	40.6	[40]
Raw beech sawdust	9.78	[41]
Garlic peel	82.64	[20]
Spent coffee grounds	18.7	[8]
Needles of <i>Pinus sylvestris</i> L.	86.96	This study

## References

- LIU Y., ZHENG Y., WANG A. Enhanced adsorption of Methylene Blue from aqueous solution by chitosan-g-poly (acrylic acid)/vermiculite hydrogel composites. *J. Environ. Sci.* **22**, (4), 486, **2010**.
- WENG C.H., PAN Y.F. Adsorption of a cationic dye (methylene blue) onto spent activated clay. *J. Hazard. Mater.* **144**, 355, **2007**.
- RAFATULLAH M., SULAIMANA O., HASHIMA R., AHMAD A. Adsorption of methylene blue on low-cost adsorbents: A review. *J. Hazard. Mater.* **177**, 70, **2010**.
- TAN I.A.W., AHMAD A.L., HAMEED B.H. Adsorption of basic dye using activated carbon prepared from oil palm shell: batch and fixed bed studies. *Desalination.* **225**, 13, **2008**.
- [http://en.wikipedia.org/wiki/Pinus\\_sylvestris](http://en.wikipedia.org/wiki/Pinus_sylvestris).
- <http://dendro.cnre.vt.edu/dendrology/syllabus/factsheet.cfm?ID=112>.
- PANIZZA M., BARBUCCI A., RICOTTI R., CERISOLA G. Electrochemical degradation of methylene blue. *Sep. Purif. Technol.* **54**, 382, **2007**.
- FRANCA A.S., OLIVEIRA L.S., FERREIRA M.E. Kinetics and equilibrium studies of methylene blue adsorption by spent coffee grounds. *Desalination.* **249**, 267, **2009**.
- HAN X., WANG W., MA X. Adsorption characteristics of methylene blue onto low cost biomass material lotus leaf. *Chem. Eng. J.* **171**, 1, **2011**.
- KUMAR P.S., RAMALINGAM S., SENTHAMARAI C., NIRANJANAA M., VIJAYALAKSHMI P., SIVANESAN S. Adsorption of dye from aqueous solution by cashew nut shell: studies on equilibrium isotherm, kinetics and thermodynamics of interactions. *Desalination.* **261**, 52, **2010**.
- SENTHILKUMAAR S., VARADARAJAN P.R., PORKODI K., SUBBHURAAM C.V. Adsorption of methylene blue onto jute fiber carbon: kinetics and equilibrium studies. *J. Colloid Interf. Sci.* **284**, 78, **2005**.
- MALKOC E. Ni(II) removal from aqueous solutions using cone biomass of *Thuja orientalis*. *J. Hazard. Mater.* **B137**, 899, **2006**.
- YU L.J., SHUKLA S.S., DORRIS K.L., SHUKLA A., MARGRAVE J.L. Adsorption of chromium from aqueous solutions by maple sawdust. *J. Hazard. Mater. B* **100**, 53, **2003**.
- DOĞAN M., ABAK H., ALKAN M. Adsorption of methylene blue onto hazelnut shell: Kinetics, mechanism and activation parameters. *J. Hazard. Mater.* **164**, 172, **2009**.
- MALKOC E., NUHOGLU Y. Determination of kinetic and equilibrium parameters of the batch adsorption of Cr(VI) onto waste acorn of *Quercus ithaburensis*. *Chem. Eng. Processing.* **46**, 1020, **2007**.
- NASUHA N., HAMEED B.H. Adsorption of methylene blue from aqueous solution onto NaOH-modified rejected tea. *Chem. Eng. J.* **166**, 783, **2011**.
- CHABANI M., AMRANEB A., BENSMALI A. Kinetic modelling of the adsorption of nitrates by ion exchange resin. *Chem. Eng. J.* **125**, 111, **2006**.
- GUPTA V.K., SUHAS I.A., SAINI V.K. Adsorption of 2,4-D and carbofuran pesticides using fertilizer and steel industry wastes. *J. Colloid Interface Sci.* **299**, 556, **2006**.
- BILGILI M.S. Adsorption of 4-chlorophenol from aqueous solutions by xad-4 resin: Isotherm, kinetic, and thermodynamic analysis. *J. Hazard. Mater.* **B137**, 157, **2006**.
- HAMEED B.H., AHMAD A.A. Batch adsorption of methylene blue from aqueous solution by garlic peel, an agricultural waste biomass. *J. Hazard. Mater.* **164**, 870, **2009**.
- MALKOC E., NUHOGLU Y. Investigations of Ni(II) removal from aqueous solutions using tea factory waste. *J. Hazard. Mater.* **127**, 120, **2005**.
- RAUF M.A., BUKALLAH S.B., HAMOUR F.A., NASIR A.S. Adsorption of dyes from aqueous solutions onto sand and their kinetic behavior. *Chem. Eng. J.* **137**, 238, **2008**.
- MALKOC E., NUHOGLU Y. Potential of tea factory waste for chromium(VI) removal from aqueous solutions: Thermodynamic and kinetic studies. *Sep. Purif. Technol.* **54**, 291, **2007**.
- NUHOGLU Y., MALKOC E. Thermodynamic and kinetic studies for environmentally friendly Ni(II) biosorption using waste pomace of olive oil factory. *Bioresource Technol.* **100**, 2375, **2009**.
- ERTUGAY N., BAYHAN Y.K. Biosorption of Cr (VI) from aqueous solutions by biomass of *Agaricus bisporus*. *J. Hazard. Mater.* **154**, 432, **2008**.
- NASUHA N., HAMEED B.H., DIN A.T.M. Rejected tea as a potential low-cost adsorbent for the removal of methylene blue. *J. Hazard. Mater.* **175**, 126, **2010**.
- MALKOC E., NUHOGLU Y. Removal of Ni(II) ions from aqueous solutions using waste of tea factory: Adsorption on a fixed-bed column. *J. Hazard. Mater.* **B135**, 328, **2006**.

28. HAN R., ZHANG L., SONG C., ZHANG M., ZHU H., ZHANG L.J. Characterization of modified wheat straw, kinetic and equilibrium study about copper ion and methylene blue adsorption in batch mode. *Carbohydr. Polym.* **79**, 1140, **2010**.
29. RYU Z., RONG H., ZHENG J., WANG M., ZHANG B. Microstructure and chemical analysis of PAN-based activated carbon fibers prepared by different activation methods. *Carbon*. **40**, 1131, **2002**.
30. OLIVEIRA L.S., FRANCA A.S., ALVES T.M., ROCHA S.D.F. Evaluation of untreated coffee husks as potential biosorbents for treatment of dye contaminated waters. *J. Hazard. Mater.* **155**, (3), 507, **2008**.
31. BANAT F., AL-ASHEH S., AL-MAKHADMEH L. Evaluation of the use of raw and activated date pits as potential adsorbents for dye containing waters. *Proc. Biochem.* **39**, 193, **2003**.
32. BANERJEE S., DASTIDAR M.G. Use of jute processing wastes for treatment of wastewater contaminated with dye and other organics. *Bioresource Technol.* **96**, 1919, **2005**.
33. UDDIN M.T., ISLAM M.A. MAHMUD, S., RUKANUZ-ZAMAN M. Adsorptive removal of methylene blue by tea waste. *J. Hazard. Mater.* **164**, 53, **2009**.
34. ANNADURAI G., JUANG R.S., LEE D.J. Use of cellulose-based wastes for adsorption of dyes from aqueous solutions. *J. Hazard. Mater.* **92**, 263, **2002**.
35. HAN R., WANG Y., HAN P., SHI J., YANG J., LU Y. Removal of methylene blue from aqueous solution by chaff in batch mode. *J. Hazard. Mater.* **B137**, 550, **2006**.
36. BULUT Y., H. AYDIN, A kinetics and thermodynamics study of methylene blue adsorption on wheat shells, *Desalination* **194**, 259, **2006**.
37. HAN R., ZHANG J., HAN P., WANG Y., ZHAO Z., TANG M. Study of equilibrium, kinetic and thermodynamic parameters about methylene blue adsorption onto natural zeolite. *Chem. Eng. J.* **145**, 496, **2009**.
38. GHOSH D., BHATTACHARYYA K.G. Adsorption of methylene blue on kaolinite. *Appl. Clay Sci.* **20**, 295, **2002**.
39. EL-HALWANY M.M. Study of adsorption isotherms and kinetic models for methylene blue adsorption on activated carbon developed from Egyptian rice hull (Part II). *Desalination*. **250**, 208, **2010**.
40. VADIVELAN V., KUMAR K.V. Equilibrium, kinetics, mechanism, and process design for the sorption of methylene blue onto rice husk. *J. Colloid Interf. Sci.* **286**, (1), 90, **2005**.
41. BATZIAS F.A., SIDIRAS D.K. Dye adsorption by calcium chloride treated beech sawdust in batch and fixed-bed systems. *J. Hazard. Mater.* **114**, (1-3), 167, **2004**.